Population inversion in plasmas generated during recombination cascades

G. J. Pert
Physics Department, University of York, Heslington, York YO10 5DD, United Kingdom
(Received 10 July 2007; revised manuscript received 4 September 2007; published 29 November 2007)

The collisional-radiative model for hydrogenlike ions is used to investigate the scaling of recombination at low temperatures in order to identify the necessary conditions of electron density and temperature, which will allow population inversion between the first excited state and the ground state to be developed. Numerical calculations show that at low temperatures the population growth in the hydrogenic states can be represented by similarity relations. The physical origin of these forms is presented. A table of minimum densities at which inversion will occur is given as a function of temperature for ions of arbitrary atomic number.

DOI: 10.1103/PhysRevE.76.056404 PACS number(s): 52.50.Jm, 42.55.Vc, 32.30.Rj, 42.60.By

I. INTRODUCTION

The generation of population inversion by recombination, and the subsequent development of gain for the extreme ultraviolet and soft x-ray spectral regions, has a long history following from the original proposal by Gudzenko and Shelepin [1]. The original applications concentrated on Balmer series transitions between the $n=2$ and higher states in the hydrogenlike sequence and in particular the $H\alpha$ line between the levels $n=2$ and $n=3$ as a result of its higher oscillator strength. Experimental evidence of this behavior in ionized systems was initially obtained by Irons and Peacock [2] and Jaeglé *et al.* [3], the latter using Li-like ions.

Analysis of the generation of gain on Lyman transitions to the ground state has been much more restricted. The potential for experiments in which the lifetime was limited by a short decay transition into the ground state and the consequent rapid ionization rate was small at that time, and only a few papers considered the problem [4–6]. More recently direct photoionization by radiation from either an adjacent laser plasma [7] or a free electron laser (FEL) [8] has been considered. In the first case electron heating resulting from a broad bandwidth of the pump radiation required further cooling to generate ground-state inversion. However, this is avoided in the second proposal by the restricted bandwidth of the tuned pump laser pulse.

The advent of short (subpicosecond) high-power laser pulses generated by chirped pulse amplification (CPA) systems changed this situation by using multiphoton ionization. Burnett and Corkum [9] introduced the concept that such lasers in linear polarization would generate very cold plasmas ideal for recombination pumping. The idea was further explored by a number of workers, principally for transitions between excited states, which can operate in a quasisteady mode. The reported experimental observation [10,11] of gain on the $L\alpha$ transition $(n=2-1)$ in a hydrogenic lithium plasma has led to a renewed interest in the possibility of lasing to the ground state in recombining systems in view of their potential to generate very short wavelengths. Theoretical studies have recently been reported by Avitzour *et al.* [12,13] and Pert [14]. In this paper we investigate this conceptual system of cold fully stripped ions in a hydrogenic background, generated by above-threshold ionization (ATI), recombining to create a population inversion between the first excited and ground states.

The general picture of cascade recombination was developed in the early 1960s where the role of the "bottleneck" in collisionally dominated systems was introduced by Hinnov and Hershberg [15] and the equivalent "collision limit" in radiatively by Griem [16] and by Kuznetsov and Raizer [17] in different forms. This model involved thermal equilibrium between the continuum and the excited states down to the bottleneck and collision limit. Recombination is due to the passage of electrons across this state, their probable subsequent trajectory being downward to the ground state. This picture was given a more formal structure in a quasiclassical analysis by Gurevich and Pitaveskii [18,19] and others [20,21] using a Fokker-Planck description. The alternative collisional-radiative scheme of Bates *et al.* [22,23] and McWhirter and Hearn [24] gives a more complete description of recombination. The two approaches were reconciled by a review of the models of recombination [25]. The Fokker-Planck equation was identified as the limit of the collisional-radiative equation for small energy differences between neighboring energy levels. The analysis also confirmed the validity of the simple physical pictures involving the bottleneck or collision limit.

This work was carried out in the 1960s and 1970s, and the scaling for collisional-radiative recombination is consequently well known. Nonetheless, despite many simulations to examine particular systems, there has been no attempt to examine the problem of inversion in a general way. In this work we will consider the population of the ground and excited states in hydrogenic ions as functions of time for a system of fixed temperature and electron density under the assumption that the free electrons have a thermal distribution. This corresponds to the experimental condition of ATI ionization of a gas mixture of mostly hydrogen, whose role is to provide a high-density cold-electron environment [26]. It will be assumed that the electron distribution is Maxwellian, although simulations indicate that there may be a cold-electron distribution, with a small hot non-Maxwellian tail [14]. It will be found that there is a general scaling which is related to that of the steady-state collisional-radiative model [24] and which allows results of considerable generality. Our principal interest will lie in transient inversion of the resonance level $n=2$ to the ground state $n=1$. The inversion therefore occurs early in the recombination of the fully stripped ions such that our assumptions of constant temperature and electron density are well maintained. If in addition a

buffer population of hydrogen ions is used to provide the cold electrons [26], this condition is even stronger.

II. MODEL

The collisional-radiative model for hydrogenic ions was developed by Bates *et al.* [22,23] and McWhirter and Hearn [24] and was extended by the author [25]. In this representation transitions between a set of hydrogenic energy levels of an ion of nuclear charge Z characterized solely by their principal quantum number n are assumed to take place due to radiative and electron collisional effects. It is assumed that no radiation absorption occurs. The population of the state n—namely, q_n—can then be written as

$$\frac{dq_n}{dt} = \sum_m C_{nm}q_m - \sum_m C_{mn}q_n + \sum_{m>n} A_{nm}q_m - \sum_{m<n} A_{mn}q_n + (C_{n\infty} + A_{n\infty})q_\infty - C_{\infty n}q_n, \tag{1}$$

where C_{mn} and A_{mn} are the electron collision and radiative transition rates from state n to state m, respectively, $C_{\infty n}$ and $C_{n\infty}$ the collisional ionization and recombination rates from and into state n, respectively, and $A_{n\infty}$ the radiative recombination rate. The fractional population of the ground state of the next ionization stage, q_∞, is given by the rate equation

$$\frac{dq_\infty}{dt} = \sum_n \{C_{\infty n}q_n - (C_{n\infty} + A_{n\infty})q_\infty\}. \tag{2}$$

The sum of Eqs. (1) and (2) is

$$\frac{d}{dt}\left(\sum_n q_n + q_\infty\right) = 0, \tag{3}$$

and the total population of the states and continuum is therefore constant.

The rates are given by relatively simple expressions, as in our earlier work [25], consistent between bound and free states:

The electron collision rate is given by the Bethe approximation [27] for excitation from state m to n $(m<n)$:

$$C_{nm} = 16\pi\left(\frac{2\pi}{3}\right)^{1/2}\frac{a_0^2 I_H^2}{W_{mn}}\left(\frac{1}{m_e kT}\right)^{1/2} \times \frac{(gf)_{mn}}{g_n}\bar{g}_{III}\exp\left(-\frac{W_{mn}}{kT}\right)n_e, \tag{4}$$

where W_{mn} is the energy difference between states n and m, I_H the ionization energy of a hydrogen atom (13.6 eV), a_0 the radius of the first Bohr orbit $(0.529\times10^{-8}$ cm), $(gf)_{mn}$ the (statistical weight)$\times$(oscillator strength) product for the transition n to m, g_n the statistical weight of state n, and n_e the electron density. Although strictly only applicable at high electron energies, a useful approximation was introduced [28,29] by assigning an empirical value for $\bar{g}_{III}$ the averaged free-free Gaunt factor to match more accurate calculations. This approach was systematically improved by Sampson and Zhang, whose final approximation for hydrogenic ions [30] we use here for both excitation and ionization.

The deexcitation rate from state m to n $(m>n)$ is given by the condition of detailed balance applied to Eq. (4):

$$C_{nm} = (g_n/g_m)C_{mn}\exp(W_{mn}/kT). \tag{5}$$

The ionization rate is obtained by extending the excitation rate to upper states for collisional excitation (4) into the continuum and integrating over the free states:

$$C_{\infty n} = \frac{2^8(2\pi)^{1/2}}{9}\frac{a_0^2 I_H}{Z^2}\frac{1}{(m_e kT)^{1/2}} \times n\bar{g}_{II}\bar{g}_{III}E_4(I_n/kT)n_e, \tag{6}$$

where I_n is the ionization energy of state n and $E_n(x)$ is the exponential integral of the nth degree.

The recombination rate into state n is also given by a condition of detailed balance applied to the ionization rate (6):

$$C_{n\infty} = \frac{h^3}{2(2\pi m_e kT)^{3/2}}\frac{g_n}{g_\infty}C_{\infty n}n_e\exp(I_n/kT). \tag{7}$$

The radiative deexcitation rate

$$A_{mn} = \frac{8\pi^2 e^2 W_{mn}^2}{m_e h^2 c^3}\frac{(gf)_{mn}}{g_n}. \tag{8}$$

The radiative recombination rate is most easily obtained by extending the above equation (8) from the bound states into the free and integrating over the continuum:

$$A_{n\infty} = \frac{128\pi^3}{3\sqrt{3}}\frac{e^2 a_0^2\alpha^3}{h}Z\left(\frac{I_n}{\pi kT}\right)^{3/2}\bar{g}_{II}\Phi\left(\frac{I_n}{kT}\right)n_e, \tag{9}$$

where h is Planck's constant, $\bar{g}_{II}$ the averaged free-bound Gaunt factor, and $\Phi(x)=e^x E_1(x)$.

A. Time-dependent model

In the transient case, the rapid depletion of the ion "reservoir" into the high-lying states occurs. The correct condition is that the total population of bound and free electrons must be held constant—i.e., Eq. (3)—which requires the integration of both Eqs. (1) and (2).

It is convenient to introduce dimensionless forms for the density and temperature:

$$Y = \frac{I_1}{kT} = \frac{Z^2 I_H}{kT},$$

$$N_e = \frac{h^3}{2(2\pi m_e kT)^{3/2}}n_e,$$

$$N_n = \frac{h^3}{2(2\pi m_e kT)^{3/2}}n_n,$$

$$N_\infty = \frac{h^3}{2(2\pi m_e kT)^{3/2}}n_\infty, \tag{10}$$

which allow the rates to be cast into a more direct form. We note that since the Fermi energy $E_F=(h^2/2m_e)(3n_e/\pi)^{2/3}$, the

expression $N_e=(1/6\sqrt{\pi})(E_F/kT)^{3/2}$, which must be small as we use classical statistics. In numerical units $N_e \approx 3.3 \times 10^{-24} Z^{-3} Y^{3/2} n_e$ (cm^{-3}), which validates the above assumption at the densities at which experiments are likely to be performed. In these units Saha's equation takes a particularly simple form

$$\frac{N_\infty N_e}{N_n} = \frac{g_\infty}{g_n} \exp(-Y/n^2). \tag{11}$$

The rates may be also cast into simpler forms in terms of a characteristic rate A,

$$A = \frac{16\pi^2 a_0^2 I_H^2 m_e}{h^3} = \frac{2I_H}{h} = 6.580 \times 10^{15}\ \mathrm{s}^{-1}, \tag{12}$$

and a constant $B=\pi\alpha^3 Z^4 = 1.221 \times 10^{-6} Z^4$. A expresses the characteristic rate of collisional processes and $\beta = B/N_e$ the relative strength of the radiative ones.

The collisional and radiative rates reduce to

$$C_{mn} \Rightarrow A\bar{C}_{mn}(Y)N_e, \tag{13}$$

$$A_{mn} \Rightarrow A\beta\bar{A}_{mn}N_e, \tag{14}$$

where

$$\bar{C}_{mn} = \frac{8\pi}{\sqrt{3}} \frac{kT}{W_{mn}} \frac{(gf)_{mn}}{g_m} \bar{g}_{III} \exp(-W_{mn}/kT), \tag{15}$$

$$\bar{C}_{\infty n} = \frac{128}{9} \frac{n}{Y} \bar{g}_{II} \bar{g}_{III} E_4(Y/n^2). \tag{16}$$

The collisional recombination rate

$$\bar{C}_{n\infty} = \frac{g_n}{g_\infty} \bar{C}_{\infty n} N_e \exp(Y/n^2), \tag{17}$$

and the radiative recombination rate

$$\bar{A}_{n\infty} = \frac{32}{3\sqrt{3}\pi} \frac{1}{n^3} \Phi(Y/n^2). \tag{18}$$

The constant A may be usefully combined with the electron density and the time to form the reduced time $\bar{t}=AN_e t$ for the collisional process, to give a modified set of equations (1):

$$\frac{dq_n}{d\bar{t}} = \sum_m \bar{C}_{nm} q_m - \sum_m \bar{C}_{mn} q_n + \sum_{m>n} \beta\bar{A}_{nm} q_m - \sum_{m<n} \beta\bar{A}_{mn} q_n + (\bar{C}_{n\infty} + \beta\bar{A}_{n\infty}) q_\infty - \bar{C}_{\infty n} q_n. \tag{19}$$

B. Steady state

The steady state, where we consider only the recombination of the system from the ionization state down to the ground state, allows a significant simplification in terms of the set of reduced variables (10) [24]. The dimensionless density forms (10) are modified to include the Z scaling and yield a set of similar relations[1]

$$\bar{N}_e = Z^{-4} N_e,$$

$$\bar{N}_n = Z^{-7} N_n,$$

$$\bar{N}_\infty = Z^{-3} N_\infty, \tag{20}$$

with the additional modifications $\bar{A}=AZ^4$ and $\bar{B}=BZ^{-4} = 1.221 \times 10^{-6}$, the other equations remaining unchanged.

If the depletion rate of the upper states is slow, we may set the population of the ionization stage to an arbitrary and constant value, typically unity, and may evaluate all the excited-state populations in terms of this. We thus eliminate the need to use Eq. (2) and simply work from the set (1) with arbitrary (unit) population in the continuum. Within the model, the total population of the high-lying excited states, which are in thermal equilibrium, may exceed that in the continuum, depending on where the (arbitrary) upper state is taken. However, in reality these states probably lie above the depressed ionization cutoff. Since these levels form a quasicontinuum in thermal equilibrium with the ionization states, this introduces no error to the overall population distribution, only changing the value of the total population, and ensures a smooth merging into the true continuum. These states make little contribution to the cascade and simply maintain a dynamic equilibrium among themselves and with the continuum. Within the model, their principal role is to establish the stochastic behavior which leads to the diffusive cascade into the lower states. Since the recombination rate is calculated as the downward flux through the states to the ground state and is the same at every level in the cascade, no error is incurred provided the value of this rate is calculated as a fraction of the ion population. Furthermore, any population inversion calculated between low-lying states is real, but the numerical value of the inversion needs to be carefully determined.

III. STEADY-STATE RECOMBINATION

At low density recombination is directly from the ionization continuum into the ground and resonance levels. The rates are given by Eq. (18). At low temperature Y is large and the function $\Phi(x) \sim 1/x$, so that the ground-state population rate is $\sim 2\times$ greater than that into the resonance level, a result which can be shown to be valid for all Y. No inversion is therefore possible unless collisional recombination plays a dominant role at least into the resonance level.

It was shown in our earlier work [25] that cascade recombination takes place in two regimes in which the cascade

[1]The scaling of $\bar{N}_n$ and $\bar{N}_\infty$ is somewhat arbitrary, governed only by the Saha relation, whereas $\bar{N}_e$ is determined by the collisional excitation rate. The choice [25] made here is that $n_e=Zn_\infty$, appropriate to a single element, but alternative forms are equally suitable [24].

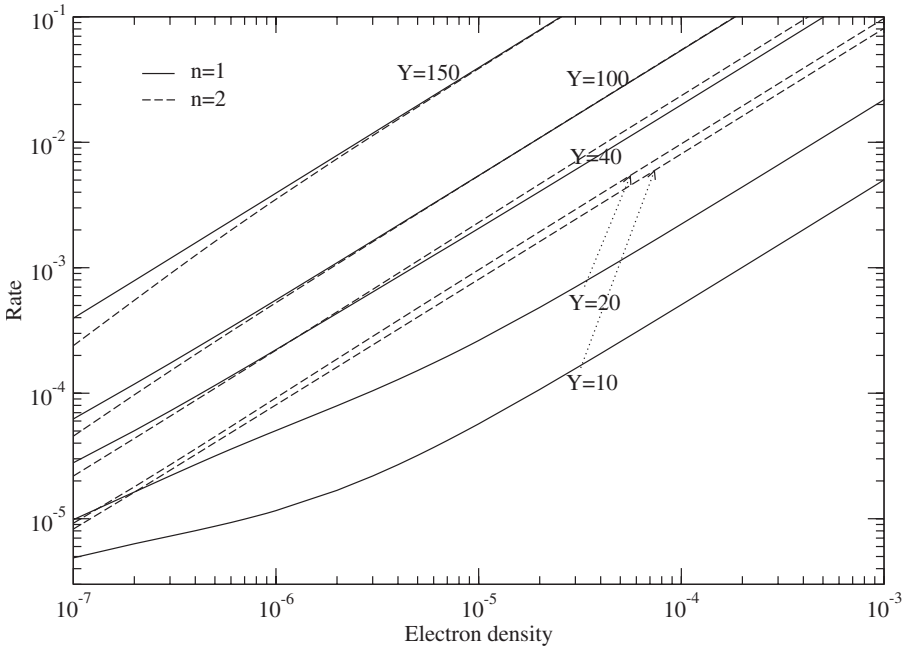

FIG. 1. Plots of the dimensionless population rates into the $n=1$ and $n=2$ states for varying electron densities ($\bar{N}_e$) and different temperatures (Y).

through the excited states is dominated by either collisional or radiative effects and depends on the larger of the two values of the lowest quantum numbers to which thermal equilibrium with the continuum can be maintained in each regime. Electrons in states below this limit probably decay to the ground state and thus contribute to recombination. In the asymptotic limit that Y is large, analytic solutions [25] allow us to clearly identify these regimes. In the collisional case this is the "bottleneck" state whose quantum number n_C is simply given by $n_C=\sqrt{Y}$. In the radiative system the limiting state is the "collision limit" given by $n_R^7[\ln n_R]^{-1}=(2/\pi^2)\bar{B}\bar{g}_{III}YN_e^{-1}$. Among the states above the appropriate limit, thermal equilibrium is maintained by strong upward collisional excitation, which balances the downward collisional and radiative deexcitation. Below the limit state this is no longer the case and it is probable that an electron will fall to the ground state, either directly or indirectly. It is not necessarily implicit that in the collisional case radiation plays no role, simply that the limit state is determined by collisional deexcitation and consequently the recombination rate also: radiative transitions are likely to play an important role in the final decay into the ground state.

It is relatively straightforward to solve the set of equations (1). The population rate of the resonance level ($n=2$) is determined by the sum of the fraction of the cascade, which passes through that level, and the direct radiative transitions from high-lying states and the continuum. Figure 1 compares the population rates into the ground and first excited states for different temperatures and densities.

We note some salient facts. At low densities the rate into the ground state is larger, a consequence of the dominance of radiative decays, which favor larger energy gaps. At high density the rate into the resonance level may be the faster, collisional effects playing a stronger role: at low temperatures collisions dominate and nearly all electrons reaching the ground state pass through the $n=2$ excited level. Below a certain temperature there is a critical density at which the two rates are equal, whose value is only weakly temperature dependent. Although low temperatures (Y large) favor collisional decay, the transition density is lower for higher temperatures (Y small).

Although we require solutions for the temporal development of the ionization and excited state populations [Eq. (1)], we can nonetheless draw some useful conclusions from these steady-state results. Since the high-lying excited states are rapidly filled, the population rates of the ground and resonance states are given approximately by the rates in Fig. 1. These show characteristic behaviors. At low density the population rate to the ground state is mainly radiative recombination, but as the density increases, the collisional cascade dominates, the transition occurring very approximately at $\bar{N}_e\sim 10^{-6}$. At high temperature ($Y\lesssim 20$) the bottleneck is sufficiently close to the $n=2$ level that upward collisional transitions from the resonance to higher levels are possible and that in the steady state the downward rate into this level is greater than that continuing down to the ground state. At low temperatures ($Y\gtrsim 50$) all downward transitions continue to the ground state. As a result, at low temperature and high density the transition rates into the ground and resonance states become nearly equal. These effects can be clearly seen in Fig. 1 for values of the temperature parameter Y greater than about 40. For values of $Y>60$ the steady-state transition rate to the resonance level never exceeds that to the ground state, the two being nearly equal for large values of the electron density $\bar{N}_e$. Any inversion under these conditions is therefore solely due to the time delays inherent in the establishment of the cascade.

To take advantage of the much larger population rates at lower temperatures to generate inversion, we must take advantage of the time delays which occur in the transient phase as the levels are progressively filled by the cascade.

IV. TRANSIENT RECOMBINATION

Turning now to the principal case of study—namely, that in which the populations of the bound states are filled by

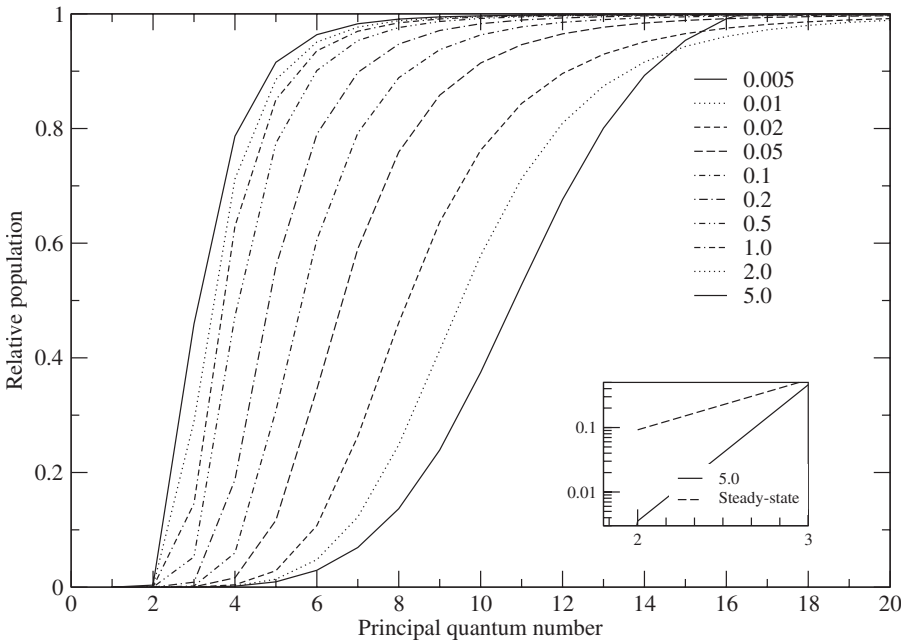

FIG. 2. Plots of the populations of the excited states scaled against the Saha population plotted for principal quantum numbers in the range 1–20 for different reduced times for the case of $Z=3$, $N_e=3\times10^{-4}$, and $Y=40$. By time 5 all states have practically reached their steady state except $n=2$ whose population is slightly too small, as shown in the inset.

recombination from the continuum—we note that the similarity with respect to Z expressed in the set of variables (20) cannot be maintained in the transient case. However, since the transient into the highly excited states is very rapid and the decay of the remaining continuum electrons slow, the decaying electrons being supplied from the large numbers in the high states, we may expect that once this early transient phase is complete, the steady state may give an accurate representation of the behavior in the higher states, and thus the Z scaling seen earlier is likely to be reasonably well obeyed.

However, this is of course an incomplete picture with respect to our problem, in that we are interested in the development of the population in both the ground and resonance states, which will themselves be strongly dependent on the progressive development to the steady-state population in the states above. Figure 2 shows the development of the populations of the excited states towards their equilibrium. Thus we see a general diffusion of population down the levels progressively filling them to their equilibrium condition. As a result, the growth of population in the levels of interest is delayed until the levels immediately above them are filled, the main transitions being collisional and therefore between neighboring levels. It can be seen that in this case a Saha population in equilibrium with the continuum is maintained down to the level $n=4$. Note that the predicted bottleneck at $n=\sqrt{Y}\approx6$ is larger than that calculated, in agreement with previous studies [25].

To demonstrate the behavior of these recombining systems we present a series of case studies, which exemplify the differences.

Figure 3 shows the recombination of lithium plasmas at three temperatures ($Y=100$, 40, and 20) and two reduced electron densities ($N_e=2\times10^{-5}$ and $N_e=3\times10^{4}$), corresponding to 1.6×10^{17} cm^{-3} and 2.45×10^{19} cm^{-3} at 1.5 eV ($Y=100$), 6.5×10^{17} cm^{-3} and 9.7×10^{18} cm^{-3} at 3 eV ($Y=40$), and 1.8×10^{18} cm^{-3} and 2.7×10^{19} cm^{-3} at 7.5 eV ($Y=20$), respectively. It can be seen that the $n=3$ level rapidly reaches its steady state, whereas the population of the $n=2$ state is still increasing slowly at the end of the calculation. It can also be seen that in every case the absolute value of the population of the $n=3$ state is practically independent of the density and the $n=2$ state almost so. The temporal histories of the $n=3$ and $n=2$ states as plotted are nearly identical for the two different densities.

In Fig. 3 the populations are plotted as fractions of their statistical weight, so that population inversion can be readily identified. At the higher density inversions are formed between the excited states and the ground state in all three cases. The relative populations are quite small and the inversion is longer lived at the highest temperature.

At the lower density the situation is changed in that at the largest value of $Y=100$—namely, the lowest temperature—no gain is achieved. At the lowest value of $Y=20$ inversion is achieved, but is relatively short lived. In the intermediate case $Y=40$ inversion is only just achieved.

Figure 4 shows a comparison of recombination in carbon with one in lithium, both at the same temperature ($Y=40$) but at different densities of $N_e=10^{-3}$ and $N_e=6.25\times10^{-5}$, respectively. The values are scaled by the factor Z^4 in accordance with the similarity expressed by the steady-state model. Comparison of two temporal profiles of population shows that they are almost exactly identical in value at a common time, but that the time history in the lithium case is slightly delayed by the initialization of the cascade.

Figure 5 also shows a case where the inversion is just formed. In this case we examine the variation with density at $Y=100$. It can be seen that an inversion is readily developed at the higher density ($n_e=2.2\times10^{20}$ cm^{-3}), but at the lower density (5.2×10^{19} cm^{-3}) one is only just formed.

V. DISCUSSION

To establish an inversion on the $L\alpha$ transition, the basic criterion is that the first excited level must fill faster than the

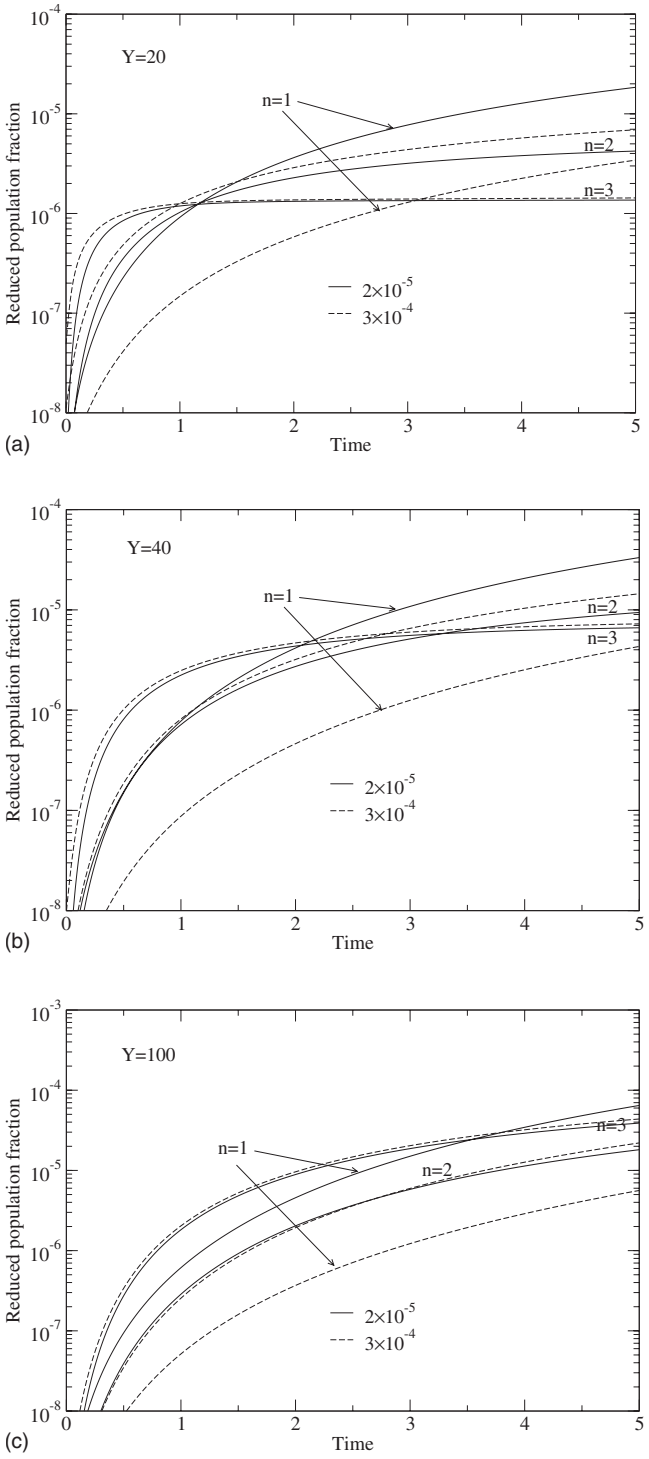

FIG. 3. Plots of the populations of the ground state and first and second excited states divided by their statistical weight plotted for principal quantum numbers as functions of the reduced time for the case of $Z=3$ at two different densities $N_e=2\times10^{-5}$ and $N_e=3\times10^{-4}$ and three different temperatures $Y=20$ (a), 40 (b), and 100 (c).

ground state. This condition requires that the recombination be dominated by collisions and that the plasma be sufficiently dense and cold that direct recombination is weak. This suggests that we operate in a collisional cascade with the bottleneck state somewhat above the first excited state, but sufficiently low that the $n=2$ level population is reasonably high—say, 50% of the Saha population—i.e., a value of $Y\sim25$. However, the Saha population in this case is itself relatively small and a larger value of Y (i.e., a lower temperature) may yield a more rapid population growth and a larger population. The time taken to establish this population distribution down to the resonance state is determined by the cascade down through the excited states. On the other hand, population growth in the ground state is normally controlled by radiation, with contributions from both the continuum and high-lying states and from the low-lying excited states (principally $n=2$ due to its large transition rate) when filled.

In these calculations the ion is represented by 200 bound states plus the continuum. This large number of levels is used to ensure that the transition between the high-lying states and the continuum is smooth. In practice, ionization depression effects will be expected to reduce the number of bound levels below this value. Typically for an ion density of 10^{19} cm^{-3}, the continuum limit is at $n\approx13$. This is well above the bottleneck so that the "diffusion" cascade is well formed in practice. The atomic states move into the continuum with similar transition rates, expressed by the local thermodynamic equilibrium (LTE) condition and Saha's equation. Use of a large number of states has replaced the continuum distribution by a closely spaced discrete one. Similar but equivalent approximations, such as forcing the upper level into Saha equilibrium with the continuum, have been used elsewhere [22–24]. The consequence of the formulation used here is that the actual continuum population is not well defined—it will depend on the position of the depressed ionization level. In a detailed calculation where the number of free electrons is reduced by recombination, this loss of electrons into the Rydberg states would present major problems. However, as we assume a constant electron density throughout the recombination, reflecting both the early stages of recombination and the nature of the physical problem considered, the use of a large number of high-lying energy levels does not lead to difficulty. This approximation allows us to identify the Z scaling, which is established very quickly as electron collisions fill in the initial void in the electron thermal distribution below the continuum. This latter process leads to an increase in the electron temperature [14] (three-body heating, not included in this analysis).

As noted earlier the time histories of the recombination as displayed show similar behavior (Figs. 3–5). The relative populations of the excited states in their steady state are constant with respect to the reduced electron density, although they vary with temperature. Due to the low temperature, most electrons are in bound high-lying states (with large statistical weight), whose populations satisfy Saha's equation. The normalization of the state populations requires that the total number of ions be constant (unity). The population among the high-lying excited states is therefore Boltzmann distributed and totals almost unity. The individual populations are consequently practically independent of density and depend only on temperature through the parameter Y. The continuum population (in this calculation) is relatively small compared to the totality of that in the excited states and (from Saha's equation) varies inversely with the electron density.

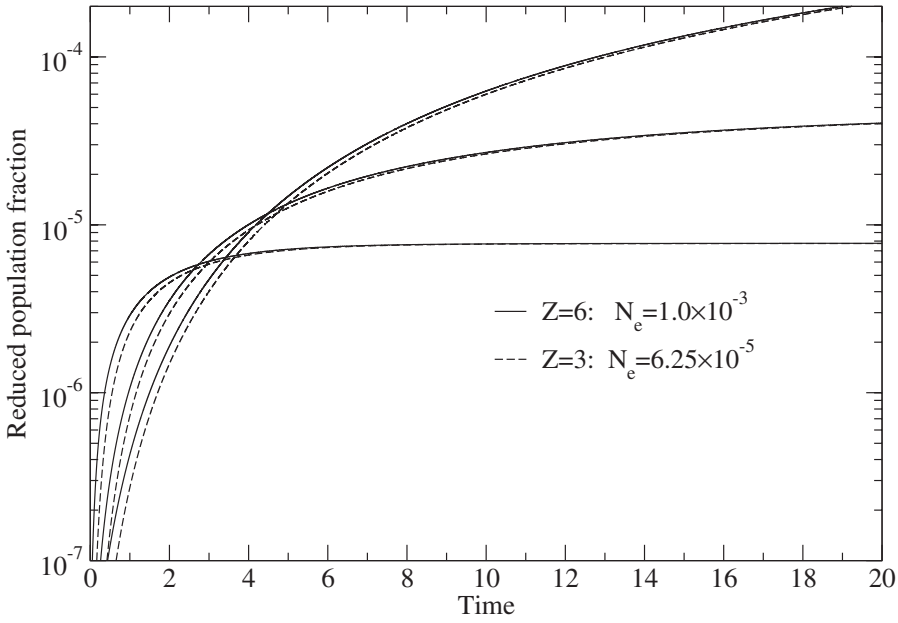

FIG. 4. Plots of the populations of the ground state and first and second excited states divided by their statistical weight plotted as functions of the reduced time for the cases of $Z=6$, $N_e=10^{-3}$ and $Z=3$, $N_e=6.25\times10^5$, and $Y=40$, illustrating the Z^4 scaling.

The reduced unit of time ($\bar{t}=AN_et$) contains the essential constants of the collision rates. Hence, since the rates are dominantly collisional among these states, the time histories of the population growth in reduced time units are independent of density. Introducing the modified radiation constant $\beta=\bar{B}/N_e$ into the reduced equations (19) we see that the equations remain unchanged if the electron density is scaled as Z^4—i.e., as in the steady state. The time histories of the states are therefore identical as noted earlier for similar values of the steady-state density parameter $\bar{N}_e$. This similarity may be expressed in a formal structure valid at low temperature:

$$q_n = q_{tot}Q_n(Z^{-4}N_e, Y, AN_et), \tag{21}$$

where q_{tot} is the total population of the ion, normally unity. The function $Q_n(\bar{N}_e, Y, \bar{t})$ can be calculated by direct integration—e.g., Figs. 3–5. For levels $n\geqslant 3$ and at very low temperatures $n=2$ also there is a further simplification $Q_n(Y,\bar{t})$ only; i.e., there is no direct dependence on $\bar{N}_e$.

This similarity relation is a consequence of the fact that, when the number of atomic states is large, nearly all the electrons are in bound states. Since the relaxation of the high-lying states with the continuum and among themselves is rapid, the steady-state relations can be applied. The number of electrons in the continuum, which has a different form, are relatively small. Hence using a set of levels cutoff at a high quantum number (200 in this case) leads to the similarity relationships. However, if a low cutoff is applied, so that the number of electrons in the continuum is relatively large, then the form of similarity is modified, such that the variables exhibiting similar behavior are $q_n/(N_eq_\infty)$ at constant Y. This term is consistent with the steady state and with the variation of q_∞ noted above, but the scaling is less exact.

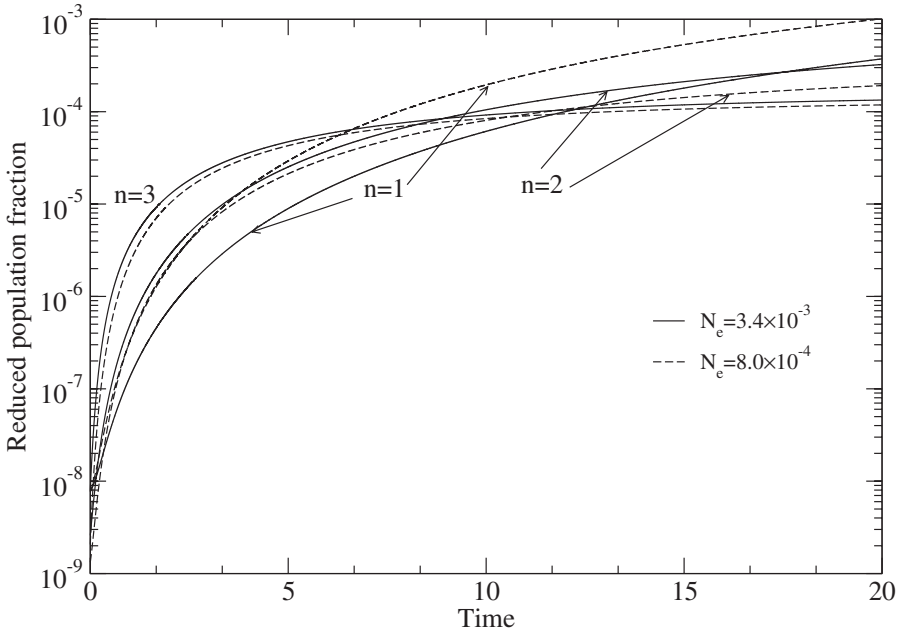

FIG. 5. Plots of the populations of the ground state and first and second excited states divided by their statistical weight plotted as functions of time for the case of $Z=6$, $N_e=8\times10^{-4}$ and $N_e=3.4\times10^{-3}$, and $Y=100$.

At "high" temperatures $Y<30$ the bottleneck lies close to the upper state of the inversion. As a result, inversions can form due to the additional net downward flux into the upper level necessary to support the population in the steady state against upward excitation. However, at low temperatures $Y>50$, the delays inherent in the development of the cascade are critical in enabling the establishment of an inversion. Following the onset of recombination the upper Rydberg levels are filled with populations in Saha equilibrium with the continuum (Fig. 2). The Saha limit progressively decreases until the bottleneck at $n=\sqrt{Y}$ is reached after about 1 time unit $(AN_e)^{-1}$. The population of the first excited state, however, achieves its equilibrium value significantly later. The growth of the $n=2$ population is quite well described by the relation

$$q_2 = \begin{cases} q_2^s\{1-\exp[-\bar{R}_2(\bar{t}-\bar{t}')\}\} & \text{if } \bar{t}>\bar{t}', \\ 0 & \text{otherwise}, \end{cases} \tag{22}$$

where $\bar{R}_2$ is the total population rate into the $n=2$ level calculated in the steady state and $\bar{t}'$ is the time taken for the higher states to reach their equilibrium values (Fig. 2). Prior to this the cascade into the level $n=2$ is weak, since the downward transitions are predominately collisional and therefore tend to be between neighboring levels. We can make an estimate of the time $\bar{t}'$ and the rate $\bar{R}_2$ from the average energy loss per unit time in the cascade [25],

$$\Delta E = \frac{8\pi}{\sqrt{3}} A Y^{-1} N_e \bar{g}_{III}, \tag{23}$$

and the ionization energy of the appropriate level. The Gaunt factor $\bar{g}_{III}$ can be estimated by comparing the analytic expression for collisional cascade recombination with the numerical calculation, in the region of interest $\bar{g}_{III}\sim 0.1$. The time (in reduced units) taken to establish the bottleneck, $\bar{t}'\sim 1$, and assuming the temperature is sufficiently high that the level n is dominantly populated by collisions $\bar{R}_n \sim n^2/Y$. At lower temperatures radiation from higher levels will dominate. A more accurate rate can be estimated from the steady-state model if necessary.

In a similar fashion, the population growth to the ground state is dominated by radiative and collisional deexcitation from the level $n=2$ immediately above and by radiative transitions from the continuum and the high-lying states. The population rate therefore increases as the level above fills, as can be seen in Fig. 3. The population is approximately described by

$$q_1 \approx \bar{R}_1 \bar{t} + \begin{cases} q_2^s \bar{R}_{12}(\bar{t}-\bar{t}')\left\{(\bar{t}-\bar{t}') - \dfrac{1-\exp[-\bar{R}_2(\bar{t}-\bar{t}')]}{\bar{R}_2}\right\} & \text{if } \bar{t}>\bar{t}', \\ 0 & \text{otherwise}, \end{cases} \tag{24}$$

where $\bar{R}_{12}$ is the total deexcitation rate from state 2 to 1 and $\bar{R}_1$ the total radiative decay rate into state 1 from high-lying states calculated from the steady-state model.

The generation of an inversion clearly depends on the relative values of the three rates $\bar{R}_1$, $\bar{R}_2$, and $\bar{R}_{12}$. Since $\bar{R}_1$ and $\bar{R}_{12}$ are predominately radiative, they are insensitive to the electron density; $\bar{R}_2$, on the other hand, is collisional. At low temperature, $q_2^s \approx \bar{R}_2/\bar{R}_{12}$, and only after time $\bar{R}_2^{-1}$ does the population rate into the ground state become $\approx(\bar{R}_1+\bar{R}_2)$. In principle, we could use this analysis to identify a criterion for the minimum density for the establishment of a population inversion. In fact, it is easier and more accurate to use simulations of the temporal development to empirically identify the limiting density. In Table I we give values of the minimum (critical) density $\bar{N}_e$ at which inversion can occur for a limited number of values of the temperature Y obtained by direct simulation in both reduced and laboratory units. It can be seen that as the temperature is reduced, the electron density is correspondingly reduced. This reflects the strong temperature dependence of the collisional cascade recombination rate $\sim T^{-9/2}$, which pumps the excited states. This should be contrasted with the radiative recombination rate directly into the ground state. However, at low density and temperature, the absolute values of the inversion density will reflect both the distance from the bottleneck and the low particle density, and may therefore be smaller than values at slightly higher temperature.

The duration of the inversion predicted from these calculations may be quite long. For example, the case of Fig. 3(b)—namely, a lithium system with $n_e=10^{19}$ cm^{-3} and $kT=3$ eV ($N_e=3\times10^{-4}$ and $Y=40$)—predicts an inversion lasting about 3.5 ps (7 units). This value may be compared the value of 1 ps [14], obtained by a calculation based on a complete (Fokker-Planck) simulation of the electron and ion population distributions following (ATI) ionization and relaxation. The difference is believed to be due to the non-Maxwellian tail of the electron distribution following ATI

TABLE I. Limiting density.

Y	20	40	100	150
$\bar{N}_e$	1.85×10^{-7}	3.09×10^{-7}	6.17×10^{-7}	8.64×10^{-7}
$Z^{-2}kT$ (eV)	0.68	0.34	0.136	0.091
$Z^{-7}n_e$ (cm^{-3})	6.27×10^{14}	3.70×10^{14}	1.87×10^{14}	1.42×10^{14}

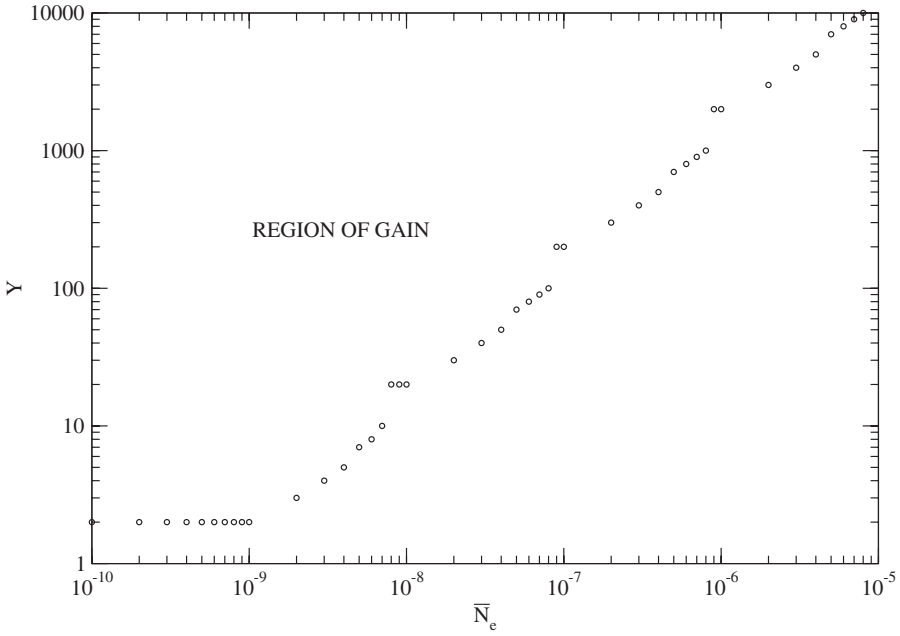

FIG. 6. Regime plot for the generation of gain on the $H\alpha$ line $n=3-2$ from the steady-state model.

associated with the ionization of hydrogenlike lithium. These electrons will reionize the $n=2$ state, damaging the inversion.

We note from Figs. 3–5 that transient inversions can also occur between the $n=3$ and the $n=1$ and 2 states—namely, on the $L\beta$ and $H\alpha$ lines. The former is of less importance than the $L\alpha$ line considered here due to its lower oscillator strength and gain, and the latter is generally developed in a quasistatic mode with longer lifetime. It is readily shown that inversions can be obtained from the steady-state model provided the $n=3$ level is dominantly pumped by collisions and the principal decay of the $n=2$ state is radiative [31].

Figure 6 shows the region within which inversions can be expected to occur on the $H\alpha$ line in the absence of radiation trapping, the region of gain lying in the upper left quadrant of the plot. The values are shown as approximations only in that no effort was made to interpolate to obtain a more accurate value. We note the near linear variation $Y \sim \bar{N}_e$. Values obtained in earlier work [32,33] are consistent with this regime.

VI. CONCLUSIONS

It is clear from Eq. (9) that the direct radiative recombination rate from the continuum into the ground state is faster than that into the resonance level. Similarly it follows from Eq. (8) that transitions from the excited states are also faster once the cascade is established. Thus population inversions between the $n=1$ and $n=2$ states cannot be generated in a purely radiative cascade system. Consequently there is a minimum density at which the inversion can occur.

Collisional population of the $n=2$ state is required to generate a ground-state–resonance-state inversion. The system must be in the collisional cascade regime, where the bottleneck lies above the collision limit. Ideally the bottleneck should lie near but above the resonance level to avoid the approach of LTE to the ground state. This implies that the temperature must be significantly less than $\frac{1}{4}Z^2 I_H$, or $Y \gtrsim 10$. The minimum density for inversion will depend on the position of the bottleneck—i.e., on the temperature.

Similarity between systems is achieved if the parameters Y and $\bar{N}_e$ are equal, provided the excited states and continuum are equilibrated after a rapid transient in which the higher states are filled to the LTE populations. The system subsequently decays in an almost quasi-steady-state mode. The minimum density condition must therefore obey this similarity form. Due to the progressive decay into the ground state, the system as a whole is inherently non-quasi-steady-state and the inversion time limited.

Population inversion can occur in the quasi-steady-state mode between the $n=2$ and higher levels, even in a radiative cascade, due to the rapid decay of the former to the ground state, provided the resonance line is optically thin.

The depressed ionization continuum limit must lie above both the resonance level for the upper laser state to exist and the bottleneck for the cascade to be well formed. The depressed ionization limit is given by $n_{lim}=1.1\times 10^4 Z^{1/2}/n_i^{1/6}$ where n_i (cm^{-3}) is the total ion density [34]. The condition on the depression of the ionization limit can thus be written as $\frac{Z}{a_0}\left(\frac{3}{4\pi n_i}\right)^{1/3} \gg \frac{I_H}{kT}$ or in scaled units $N_i Y^{3/2} \gg 1/3$.

The increasing strength of radiative transitions with respect to collisional (B), as the atomic number Z increases, limits the onset of inversion at high Z. At large atomic numbers, Z, the onset of degeneracy inhibits recombination when the value of $\bar{N}_e \lesssim 0.01 Z^{-4}$, implying a value Y, which may be too small to allow inversion.

It is implicit in this model that the plasma be dilute (weakly coupled), so that the interionic separation distance $0.62 n_i^{-1/3}$ will be small compared to the Debye length $743\sqrt{kT/n_e}$ in cgs units with kT in eV or in scaled units $1.4 Z^{-3/4} Y^{1/4} N_i^{-1/3} N_e^{1/2} \ll 1$.

APPENDIX: SIMILARITY RELATIONS

Relaxation among the higher excited states and the continuum is very rapid compared to the rate of population of the lower states. The population among the upper states is therefore given approximately by their steady-state values with respect to the continuum—i.e., modified Saha populations—such that the continuum population can be written

$$q_\infty = 1 \Big/ \left[1 + N_e \sum \phi_n g_n \exp(Y/n^2) \right], \tag{A1}$$

where $\phi_n(Y,\overline{N_e})$ is the Saha correction term for level n and $\bar{N}_e = Z^{-4} N_e$.

For short times such that the population of the lower levels remains small and assuming that the population of the upper levels is sufficiently large, the continuum population q_∞ may be considered constant. The population of level n, q_n, is expressed as $f_n = q_n/(q_\infty N_e)$. Thus the growth of the population of level n in our reduced units can be expressed as

$$\frac{df_n}{d\bar{t}} = \sum \bar{C}_{nm}(Y) f_m - \bar{C}_{mn}(Y) f_n + \sum_{m>n} \beta \bar{A}_{nm} f_m - \sum_{m<n} \beta \bar{A}_{mn} f_n + [\tilde{C}_{n\infty}(Y) + \beta \tilde{A}_{n\infty}(Y)] - \bar{C}_{\infty n}(Y) f_n, \tag{A2}$$

where $\tilde{C}_{n\infty} = \bar{C}_{n\infty}/N_e$ and $\tilde{A}_{n\infty} = \bar{A}_{n\infty}/N_e$. Noting that $\beta = 1.221 \times 10^{-6}/\bar{N}_e$ we see that

$$f_n(Y, \overline{N_e}, \bar{t}).$$

Furthermore, if the number of excited levels is large or the density high and temperature low, it follows from Eq. (A1) that $N_e q_\infty$ is a function of Y and $\bar{N}_e$ only and hence that $q_n(Y, \bar{N}_e, \bar{t})$ only, as discussed earlier.

[1] L. I. Gudzenko and L. A. Shelepin, Sov. Phys. Dokl. **10**, 147 (1969).
[2] F. E. Irons and N. J. Peacock, J. Phys. B **7**, 1109 (1974).
[3] P. Jaeglé, G. Jamelot, A. Carillon, A. Sureau, and P. Dhez, Phys. Rev. Lett. **33**, 1070 (1974).
[4] J. Peyraud and N. Peyraud, J. Appl. Phys. **43**, 2993 (1972).
[5] W. W. Jones and A. W. Ali, J. Appl. Phys. **48**, 3118 (1977).
[6] G. J. Tallents, J. Phys. B **10**, 1769 (1977).
[7] D. Goodwin and E. Fill, J. Appl. Phys. **64**, 1005 (1988).
[8] K. Lan, E. Fill, and J. Meyer-ter-Vehn, Europhys. Lett. **64**, 454 (2003).
[9] N. Burnett and P. Corkum, J. Opt. Soc. Am. B **6**, 1195 (1989).
[10] Y. Nagata, K. Midorikawa, S. Kubodera, M. Obara, H. Tashiro, and K. Toyoda, Phys. Rev. Lett. **71**, 3774 (1993).
[11] D. V. Korobkin, C. H. Nam, S. Suckewer, and A. Goltsov, Phys. Rev. Lett. **77**, 5206 (1996).
[12] Y. Avitzour, S. Suckewer, and E. Valeo, Phys. Rev. E **69**, 046409 (2004).
[13] Y. Avitzour and S. Suckewer, J. Opt. Soc. Am. B **23**, 925 (2006).
[14] G. J. Pert, Phys. Rev. E **73**, 066401 (2006).
[15] E. Hinnov and J. Hirshberg, Phys. Rev. **125**, 795 (1962).
[16] H. Griem, *Plasma Spectroscopy* (McGraw-Hill, New York, 1964).
[17] N. M. Kuznetsov and Yu. P. Raizer, J. Appl. Mech. Tech. Phys. **4**, 6 (1965).
[18] L. Pitaevskii, Sov. Phys. JETP **15**, 913 (1962).
[19] A. V. Gurevich and L. P. Pitaevskii, Sov. Phys. JETP **19**, 870 (1964).
[20] V. A. Abramov and B. M. Smirnov, Opt. Spectrosc. **21**, 9 (1966).
[21] I. S. Veselovskii, Sov. Phys. Tech. Phys. **14**, 193 (1969).
[22] D. Bates, A. Kingston, and R. McWhirter, Proc. R. Soc. London, Ser. A **270**, 155 (1962).
[23] D. Bates, A. Kingston, and R. McWhirter, Proc. R. Soc. London, Ser. A **279**, 10 (1963).
[24] R. McWhirter and A. Hearn, Proc. Phys. Soc. London **82**, 641 (1962).
[25] G. Pert, J. Phys. B **25**, 619 (1990).
[26] M. Grout, K. Janulewicz, S. Healy, and G. Pert, Opt. Commun. **141**, 213 (1997).
[27] L. Landau and E. Lifshitz, *Quantum Mechanics* (Pergamon Press, Oxford, 1959).
[28] H. van Regemorter, Astron. J. **136**, 906 (1962).
[29] M. Seaton, in *Atomic and Molecular Processes*, edited by D. Bates (Academic Press, New York, 1962), pp. 375–420.
[30] D. Sampson and H. Zhang, Astrophys. J. **335**, 516 (1988).
[31] G. Pert and S. Ramsden, Opt. Commun. **11**, 270 (1974).
[32] G. Pert, J. Phys. B **9**, 3301 (1975).
[33] D. Jacoby, G. J. Pert, L. D. Shorrock, and G. J. Tallents, J. Phys. B **15**, 3557 (1982).
[34] R. M. More, Adv. At. Mol. Phys. **21**, 305 (1986).